





## Article

# Influence of the Nitrided Layer Structure on the Micro-Pitting and Wear Behavior of Slow-Running Nitrided External Gears

Stefanie Hoja <sup>1,\*</sup>, Michael Geitner <sup>2</sup>, Bernd Zornek <sup>3,†</sup>, Franz Hoffmann <sup>4,‡</sup>, Thomas Tobie <sup>2</sup>, Karsten Stahl <sup>2</sup> and Rainer Fechte-Heinen <sup>1,5</sup>

<sup>1</sup> Leibniz-Institut für Werkstofforientierte Technologien—IWT, 28359 Bremen, Germany; fechte@iwt-bremen.de  
<sup>2</sup> Gear Research Center (FZG), Technical University of Munich, 85748 Garching, Germany; michael.geitner@tum.de (M.G.); thomas.tobie@tum.de (T.T.); karsten.stahl@tum.de (K.S.)  
<sup>3</sup> Magna PT B.V. & Co. KG, 74199 Untergruppenbach, Germany; zornek.bernd@googlemail.com  
<sup>4</sup> Professor Hoffmann Werkstofftechnik, 28757 Bremen, Germany; info@phwt-bremen.de  
<sup>5</sup> MAPEX Center for Materials and Processes, University of Bremen, 28359 Bremen, Germany  
\* Correspondence: shoja@iwt-bremen.de  
† Former member of FZG.  
‡ Former member of IWT.

**Abstract:** Nitriding can significantly increase the load carrying properties of gears. While the diffusion layer is primarily responsible for improving the tooth root and flank load carrying capacity, the compound layer mainly determines the tribological properties of the gear surface. In the present work, the influence of the compound layer on the tribological load carrying capacity of nitrided gears in the N/N pairing was investigated. For this purpose, compound layers with different thickness, porosity and phase composition were produced and their micro-pitting and wear behavior were investigated in load stage and speed stage tests. The test results confirm that the properties of the compound layer are decisive for the micro-pitting and wear resistance of nitrided gears. For a high micro-pitting resistance, the presence of pores in the near-surface area of the compound layer is of high importance, since no micro-pitting occurred as long as pores were present. With regard to the wear behavior, no dependence on the compound layer thickness or the porous zone thickness was found while the phase composition of the compound layer shows a decisive influence.

**Keywords:** nitriding; nitrocarburizing; compound layer; external gearing; tribological load carrying capacity; micro-pitting; wear



**Citation:** Hoja, S.; Geitner, M.; Zornek, B.; Hoffmann, F.; Tobie, T.; Stahl, K.; Fechte-Heinen, R. Influence of the Nitrided Layer Structure on the Micro-Pitting and Wear Behavior of Slow-Running Nitrided External Gears. *Lubricants* **2022**, *10*, 88. <https://doi.org/10.3390/lubricants10050088>

Received: 18 January 2022

Accepted: 29 April 2022

Published: 6 May 2022

**Publisher's Note:** MDPI stays neutral with regard to jurisdictional claims in published maps and institutional affiliations.



**Copyright:** © 2022 by the authors. Licensee MDPI, Basel, Switzerland. This article is an open access article distributed under the terms and conditions of the Creative Commons Attribution (CC BY) license (<https://creativecommons.org/licenses/by/4.0/>).

## 1. Introduction

Nitriding is used to achieve properties such as high surface hardness, increased fatigue strength and high wear and corrosion resistance [1,2]. During nitriding, the surface layer is enriched with nitrogen at temperatures of 480–520 °C. The nitrogen is initially dissolved in the ferrite; as the nitrogen concentration in the surface layer increases, iron nitrides are precipitated in the ferritic matrix as soon as the maximum nitrogen solubility in the ferrite is exceeded. With increasing nitriding time, the iron nitrides grow together at the surface to form a closed compound layer a few micrometers thick. In the outer area of the compound layer, pores may form due to the recombination of atomic nitrogen to molecular nitrogen at high nitrogen concentrations. The nitrogen-enriched area below the compound layer is called diffusion layer (or precipitation layer) and usually reaches several hundred micrometers deep into the material. While the diffusion layer contributes to the improvement of the mechanical properties, in particular the component load carrying capacity under oscillating stress, the compound layer is mainly responsible for the wear and corrosion behavior of the component. Various wear model studies on nitrided specimens show that the compound layer plays a greater role in micro-pitting behavior and wear than the nitriding hardness depth [3,4].

The compound layer, which is only a few micrometers thick and forms at the component surface during nitriding, usually consists of the iron nitrides  $\text{Fe}_4\text{N}$  ( $\gamma'$ -nitride) and  $\text{Fe}_{2-3}\text{N}$  ( $\epsilon$ -nitride) as well as alloying element nitrides. These nitride precipitations have a high hardness and increase the wear resistance of the component's surface. As the proportion of  $\epsilon$ -nitride increases, so does generally the wear resistance of the compound layer. In addition to the higher hardness, the  $\epsilon$ -nitride has a more favorable crystal structure than the  $\gamma'$ -nitride: the hexagonal structure has a low number of sliding systems, which together prevent the two-dimensional approach of the wear partners down to atomic distances. For this reason, the adhesion tendency of  $\epsilon$ -nitride layers is low [5].

The microstructure of the compound layer also affects the wear behavior; both the pore content and the pore distribution and size have an influence. Pores can absorb lubricant, so that the porous zone represents a lubricant depot in case of missing or insufficient lubrication. More likely is the theory that, due to the porous surface and depending on the wear conditions, an increased initial wear occurs until an optimum form fit and a higher load carrying ratio on the surface has been established with the wear partners sliding on each other [6].

Nitriding can significantly increase the load carrying capacity of gears compared to the quenched and tempered initial condition. Previous investigations on nitrided gears focused mainly on the tooth flank and tooth root load carrying capacity. However, within the experimental tests on the flank load carrying capacity by Schlötermann [7], micro-pitting in the area of negative sliding was found in almost all variants. Furthermore, pitting and spallings occurred and in some cases the flank surface was completely destroyed. In the investigations on the flank load carrying capacity by Günther, Pouteau and Bruckmeier [8], micro-pitting also appeared as a significant form of damage. As soon as there is no longer an intact compound layer, micro-pitting and severe wear as well as subsequent pitting limit the service life of nitrided gears.

Schönnenbeck [9] observed that in gas-nitrided gears micro-pitting occurred only at very high pressures. This micro-pitting was preceded by damage to the compound layer. As long as the compound layer was undamaged, the test gears were insensitive to micro-pitting. In the micro-pitting test performed by Emmert [10], no micro-pitting could be generated with the gas-nitrided specimens. However, the subsequent endurance run had to be terminated due to pitting. The tests were performed at medium and high circumferential speeds  $v_t = 8.3$  m/s and  $v_t \geq 16$  m/s, respectively. Here, the test gears were nitrided in accordance with the state of the art (at that time) using classic gas nitriding.

Bull [11] investigated the influence of the compound layer on the micro-pitting behavior of nitrided gears in comparison with case-hardened gears. It was found that the compound layer created by the nitriding process gives the gears an adequate micro-pitting resistance. Among the possible reasons for the improved micro-pitting behavior compared to case-hardened gears, Bull cites improved running-in behavior of the compound layer. Roughness peaks are preferentially removed, which produces an effect similar to vibratory grinding. Bull also observed on case-hardened gears that micro-pitting leads to a branching of the cracks starting from the surface. This could not be observed on the nitrided gears.

Other recent studies on the subject of nitriding are mainly concerned with optimizing the fatigue strength (pitting and tooth root breakage) for small and medium sized gears in comparison with case hardening. The results also show that a high flank load capacity of nitrided gears is given as long as the compound layer on the surface is intact. If the compound layer is damaged, the service life is limited by wear, micro-pitting and/or pitting [12–16].

The increase in performance, for example in the field of wind turbine gearboxes, has increased the risk of flank damages due to unfavorable tribological conditions, especially such as wear and micro-pitting. Nitriding to increase the wear resistance is therefore becoming increasingly important, especially for low-speed running conditions. Due to low circumferential speeds, the tooth flanks are subject to special requirements in terms of

the tribological load carrying capacity of the surface, while the pitting and tooth root load carrying capacity of the quenched and tempered base material is usually sufficient.

Modern nitriding processes, such as controlled gas nitriding or plasma nitriding, allow the layer properties to be adjusted by controlling the nitriding parameters during heat treatment. By a suitable choice of temperature, duration and nitriding potential, the compound layer thickness and its nitride phase composition can be specifically adjusted. Even suppression of compound layer formation is possible [5]. Which layer or surface properties are particularly advantageous with regard to the tribological load carrying capacity of nitrided gears has not yet been sufficiently clarified. According to the standards DIN 3990 5 [17] and ISO 6336-5:2003 [18], a compound layer thickness of  $CLT \leq 25 \mu\text{m}$  and a high proportion of  $\epsilon$ -nitride ( $\epsilon/\gamma' > 8$ ) is recommended for material quality ME (regarding pitting and tooth root load carrying capacity). For the current version ISO 6336 5:2016 [19], the recommended ratio of the compound layer phases is reverse ( $\gamma'/\epsilon > 8$ ). The aim of the present investigations was therefore to determine the effects of the structure of the compound layer on the tribological load carrying capacity for slow-running nitrided gears.

## 2. Materials and Methods

### 2.1. Material and Heat Treatment

The nitriding and quenching and tempering steel 31CrMoV9, which is frequently applied for nitrided gears, was used for the test gears within the experimental investigations. The chemical composition of the material batch determined by optical emission spectroscopy (OES) is shown in Table 1. The material was supplied with a quenched and tempered strength of  $1031 \text{ N/mm}^2$  ( $900 \text{ }^\circ\text{C}/\text{water} + 630 \text{ }^\circ\text{C} \text{ 2 h air} + 610 \text{ }^\circ\text{C air}$ ).

**Table 1.** Chemical composition (in mass %) of the test material 31CrMoV9 (1.8519).

Source	C	Si	Mn	P	S	Cr	Mo	V
ISO 683-5	0.27–0.34	max. 0.40	0.40–0.70	max. 0.025	max. 0.035	2.30–2.70	0.15–0.25	0.10–0.20
OES	0.31	0.24	0.67	0.010	0.014	2.48	0.22	0.16

The reference variant was nitrided according to current industrial standards at an industrial hardening shop. The test gears were gas-nitrided at a temperature of  $510 \text{ }^\circ\text{C}$  for 30 h.

Nitriding and nitrocarburizing treatments to vary the compound layer were performed in a gas nitriding system with nitriding and carburizing potential control. Heating was performed under ammonia atmosphere to activate the sample surface. Cooling after nitriding was also carried out with the addition of ammonia (phase-controlled cooling) to avoid nitrogen effusion and subsequent denitriding at the end of the process.

Three treatments were carried out for the investigations, in which essentially the composition and thickness of the compound layer were varied (with approximately the same nitriding hardness depth as the reference variant). The treatment variants VS1 and VS2 were carried out at  $520 \text{ }^\circ\text{C}$  for 42 h. Different nitriding potentials ( $K_N = 1$  and  $K_N = 3$ ) were used to vary the thickness and phase composition of the compound layer. As a further variant, nitrocarburizing with a nitriding potential of  $K_N = 1$  and a carburizing potential of  $K_C^B = 0.1$  was carried out to achieve a significantly higher proportion of  $\epsilon$ -(carbo-)nitride in the compound layer. Due to the higher treatment temperature of  $550 \text{ }^\circ\text{C}$  required for nitrocarburizing, a somewhat lower strength of the diffusion layer can be expected with this variant. The nitrocarburizing time was reduced to 21 h due to the higher treatment temperature in order to achieve a similar nitriding hardness depth as the reference.

The evaluation of the compound layer and the porous zone of the compound layer was carried out according to DIN 30902:2016-12 [20] on the metallographic cross-section, which was taken by spark erosion on an untested gear flank following the gear running tests. All sections were etched with Nital and images were taken at 1000x magnification. Mean compound layer and porous zone thickness were determined by measuring at ten

locations on three micrographs. In addition with the documentation of the compound layer, the nitriding hardness depth and core hardness were also determined on the cross-section. The core strength was converted from the core hardness according to ISO 18265 [21]. The hardness of the compound layer and the porous zone were determined with the instrumented indentation test. The chosen test force of 5 mN corresponds to the smallest possible force in order to achieve the most local testing possible.

The composition of the compound layers was determined by radiographic methods. From X-ray diffraction spectra recorded with Cr- $K_{\alpha}$  radiation, the proportions of  $\epsilon$ - and  $\gamma'$ -nitride were determined according to the Rietveld method [22] by considering the entire spectrum to be a mathematical function of the diffraction angle, which also depends on the crystal structure. Starting from an initial model of the atomic ordering, structural and instrumental parameters are refined more and more. The penetration depth of the X-rays defined as the depth to the drop of the radiation intensity to  $e^{-1}$  is limited to approx. 10  $\mu\text{m}$  and the information about the phase fractions is included in the measured value weighted according to depth in accordance with an exponential function. Therefore the information obtained in this way can be seen as the average phase composition in the case of thicker compound layers.

## 2.2. Test Gears

The FZG (Forschungsstelle für Zahnräder und Getriebesysteme/Gear research center, TU Munich) standard gear geometry type C was used for the experimental investigations. The relevant main geometry data of the test gears are summarized in Table 2.

**Table 2.** Main geometry data of the test gears.

Parameter	Unit	Type C (External Gears)		
		Pinion	Wheel	
Normal module	$m_n$	mm	4.5	
Number of teeth	$z$	-	16	24
Face width	$b$	mm	14.0	
Normal pressure angle	$\alpha_n$	$^{\circ}$	20.0	
Working pressure angle	$\alpha_{wt}$	$^{\circ}$	22.44	
Helix angle	$\beta$	$^{\circ}$	0	
Transverse contact ratio	$\epsilon_{\alpha}$	-	1.436	
Addendum modification coefficient	$x$	-	0.1817	0.1715
Reference diameter	$d$	mm	72.0	108.0
Tip circle diameter	$d_a$	mm	82.5	118.4
Center distance	$a$	mm	91.5	

The nitrided test gears were finish ground prior to nitriding and subsequently not machined. All test gears were ground with a short involute tip relief ( $C_a = 25 \pm 5 \mu\text{m}$ ). To counteract edge bulges caused by nitriding and its effects during operation, an additional end relief ( $C_e = 12.5 \pm 2.5 \mu\text{m}$ ) was applied to the test gears before nitriding. The influences of this modified pressure distribution compared to uncorrected gears were taken into account via the face load factor  $K_{H\beta}$  according to ISO 6336-1 [23], the details are documented in [24].

The roughness of the test gears before nitriding was  $R_a = 0.23 \mu\text{m}$  on average. Nitriding resulted in a slight increase in roughness to an average of  $R_a = 0.32 \mu\text{m}$ .

In the nitrided condition, most of the test gears showed gear tooth qualities  $Q \leq 5$  according to DIN 3963 [25]. Before nitriding, the test gears showed negative profile angle deviations with qualities of  $Q \leq 7$ . Nitriding shifted these deviations in a positive direction, which did not significantly change the quality in terms of profile shape. The quality of the flank shape of almost all test gears was in the range  $Q \leq 5$  before nitriding. However, nitriding resulted in some cases in significant inverse crowning and thus in a degradation

of the quality. On average, nitriding resulted in a degradation of the gear tooth quality by approx. 1–2 quality grades.

### 2.3. Gear Testing

The gear running tests were carried out on FZG back-to-back test rigs with a center distance of  $a = 91.5$  mm (see Figure 1). This is a cylindrical gear test rig with a closed power circuit. The static moment applied by the loading clutch by means of a load lever and defined weights is transmitted via the test gear set and the usually helical-toothed drive gear set. During operation, only the power loss is supposed to be supplied by the electric motor into the bracing circuit. In the test gear box, the pinion drives the wheel. For the herein presented investigations on the micro-pitting and low-speed wear behavior, a continuously variable motor with an additional switchable countershaft transmission between the motor and the drive gear box was used to ensure low circumferential speeds of  $v_t \leq 2$  m/s.

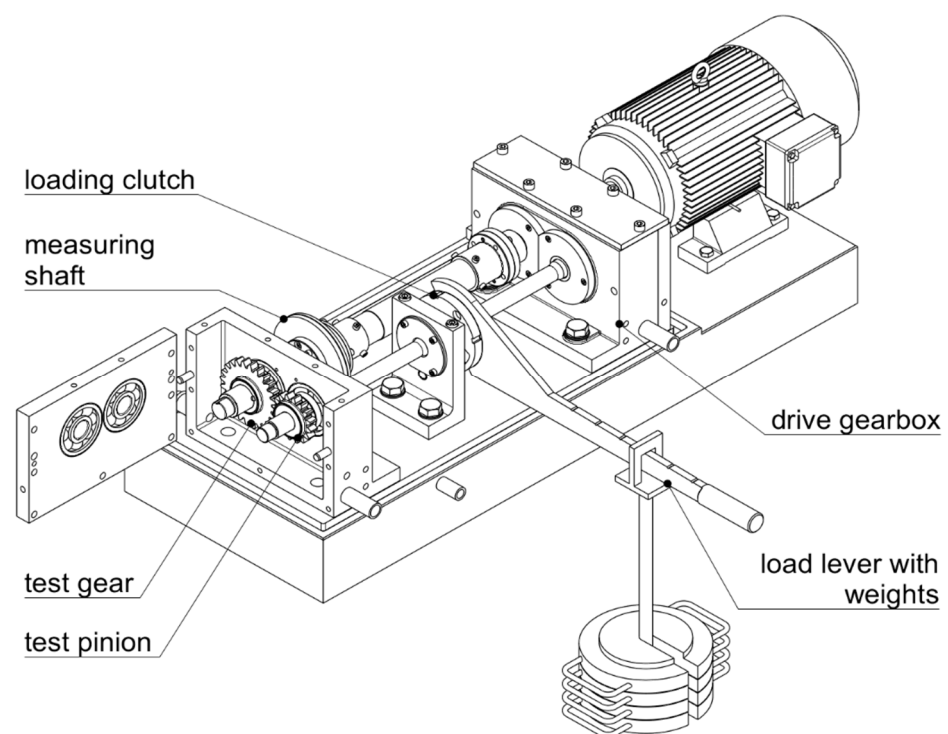


**Figure 1.** FZG back-to-back test rig (schematic) based on DIN ISO 14635-1 [26].

The micro-pitting behavior of the investigated variants (see Table 3) was determined by load stage tests performed according to FVA 482/I [27]. In order to obtain comparative information on the micro-pitting behavior of the different compound layer variants, the load was increased stepwise at a constant circumferential speed of  $v_t = 2$  m/s. The load stages (BS) were selected based on the standard micro-pitting test according to FVA 54/7 [28]. The effects of the deviating microgeometry of the test gears (end relief) were taken into account via the face load factor  $K_{H\beta}$  according to ISO 6336-1 [23] ( $p_C^* = p_C \cdot \sqrt{K_{H\beta}}$ ), the torque levels within the tests were adjusted accordingly. The load was increased starting at BS 8 ( $p_C^* = 1100$  N/mm<sup>2</sup>) up to BS 13 ( $p_C^* = 1850$  N/mm<sup>2</sup>). The running time per load stage interval was 16 h. All tests were carried out with injection lubrication using the reference lubricant FVA 3 (mineral oil of viscosity grade ISO VG 100) + 4% Anglamol 99 at an oil injection temperature of  $\vartheta_{oil} = 60$  °C. A second test run was carried out for all variants to validate the results.

**Table 3.** Overview of the nitrided layer properties of the investigated test gears.

Variant	NHD <sub>400HV</sub> in mm	CLT in µm	CLT <sub>P</sub> in µm	Core Hardness in HV10	Core Strength * in N/mm <sup>2</sup>	Phases in the Compound Layer
R (reference) 510 °C 30 h	0.38	11.4	3.7	276	861	56% ε-nitride 35% γ'-nitride 9% cementite
VS1 520 °C 42 h K <sub>N</sub> = 1	0.43	4.1	0.5	326	1020	100% γ'-nitride
VS2 520 °C 42 h K <sub>N</sub> = 3	0.53	12.6	4.5	327	1020	15% ε-nitride 85% γ'-nitride
NC 550 °C 21 h K <sub>N</sub> = 1 K <sub>C</sub> <sup>B</sup> = 0.1	0.43	17.6	4.3	321	1003	47% ε-nitride 53% γ'-nitride

\* converted according to ISO 18265.

In the speed stage test, the load was kept constant, while the circumferential speed was varied stepwise from speed stage GS 1 ( $v_t = 2$  m/s) to GS 7 ( $v_t = 0.05$  m/s) to determine the (micro-pitting and) wear behavior. The speed stage tests were carried out at  $p_C^* = 1850$  N/mm<sup>2</sup>. All tests were carried out at injection lubrication with the unadditivated lubricant FVA 3 and an oil temperature of  $\vartheta_{oil} = 60$  °C. Similarly to the load stage tests, a second test run was carried out for each variant to increase the reliability of the test results. Due to damages in the compound layer on the tooth flanks of the test gears in almost all variants, the mass loss was only evaluated for the test pinions. The running time per speed stage interval was 16 h. For the presentation of the mass loss, the wear amounts were converted to the same number of load cycles (100,000 load cycles on the test pinion), assuming a linear wear behavior in each interval.

During the experimental investigations, spalling of the compound layer respectively white layer flaking starting from the tip edge of the nitrided test wheels (beginning of contact) was observed in some variants. However, the applied tip relief on the test wheels was not designed for optimum load carrying capacity at very high loads. For practical application, it is therefore necessary to design the micro-geometry modifications in such a way that both the tip edges and the face edges of the nitrided gears are relieved in a suitable way.

#### 2.4. Determination of the Wear Behavior

According to Plewe [29], the lubricant film thickness  $h_{C,min}$  at the pitch point C (see Formula (1), based on Dowson [30]) is used as the decisive parameter for wear on gears:

$$h_{C,min} = 2.65 \cdot \rho_C \cdot (\alpha \cdot E')^{0.54} \cdot \left( \frac{\eta_0 \cdot v \cdot \sin \alpha_w}{E' \cdot \rho_C} \right)^{0.7} \cdot \left( \frac{2 \cdot T \cdot 10^9}{d_b \cdot b \cdot E' \cdot \rho_C} \right)^{-0.13} \quad (1)$$

$h_{C,min}$ : Minimum lubricant film thickness in C

$\rho_C$ : Radius of relative curvature in C

$\alpha$ : Pressure-viscosity coefficient

$E'$ : Relative modulus of elasticity

$\eta_0$ : Dynamic viscosity at bulk temperature

$v$ : Kinematic viscosity

$\alpha_w$ : Working pressure angle

$T$ : Applied torque

$d_b$ : Base diameter

$b$ : Gear face width

Depending on the material pairing, Plewe [29] gives the following reference values of the minimum permissible lubricant film thickness  $h_{C,min,per}$  for unalloyed lubricants as a parameter to specify an operating range at risk of wear.

Material pairings of the same surface hardness are characterized by a risk of wear for lubricant film thicknesses below  $h_{C,min,per} = 0.05$  µm.

In the case of the material pairing hard/soft, service life-limiting wear on the softer gear can be expected with lubricant film thicknesses up to  $h_{C,min,per} = 0.4 \mu\text{m}$ .

According to Plewe [29], a linear wear coefficient  $c_{IT,Plewe}$  is determined on the basis of the mass loss  $W_m$  measured in the test:

$$c_{IT,Plewe} = \frac{W_m}{2 \cdot b \cdot m_n \cdot z \cdot \rho \cdot N} \quad (2)$$

$c_{IT,Plewe}$ : Linear wear coefficient

$W_m$ : Mass loss

$b$ : Gear face width

$m_n$ : Normal module

$z$ : Number of teeth

$\rho$ : Density

$N$ : Applied load cycles

The investigations on the wear behavior carried out here deviate with regard to the load ( $\sigma_{H0,test} = 1710 \text{ N/mm}^2$ ) from the tests carried out by Plewe [29] ( $\sigma_{H0,Plewe} = 1160 \text{ N/mm}^2$ ), but relevant geometry sizes can be adopted due to the use of the same test gear main geometry (type C: radius of relative curvature in pitch point  $\rho_C = 8.38 \text{ mm}$ , wear-effective specific sliding  $\zeta_W = 0.739$ ). A classification of the wear coefficients according to Plewe is therefore only possible here after a corresponding reevaluation. A reevaluation of results with different test conditions is possible according to Formula (3) on the basis of the nominal contact stress, the radius of relative curvature and the wear-effective specific sliding. The parameters  $\sigma_{H0,Plewe}$ ,  $\rho_{C,Plewe}$  and  $\zeta_{W,Plewe}$  refer to the test conditions according to Plewe, the parameters  $\sigma_{H0,test}$ ,  $\rho_{C,test}$  and  $\zeta_{W,test}$  to the tests carried out here:

$$c_{IT} = \frac{W_m}{2 \cdot b \cdot m_n \cdot z \cdot \rho \cdot N} \cdot \left( \frac{\sigma_{H0,Plewe}}{\sigma_{H0,test}} \right)^{1.4} \cdot \left( \frac{\rho_{C,Plewe}}{\rho_{C,test}} \right) \cdot \left( \frac{\zeta_{W,Plewe}}{\zeta_{W,test}} \right) \quad (3)$$

$c_{IT}$ : Linear wear coefficient, reevaluated regarding the test conditions acc. to Plewe

$W_m$ : Mass loss

$b$ : Gear face width

$m_n$ : Normal module

$z$ : Number of teeth

$\rho$ : Density

$N$ : Applied load cycles

$\sigma_{H0,Plewe}$ : Nominal contact stress referring to the test conditions acc. to Plewe

$\sigma_{H0,test}$ : Nominal contact stress referring to the carried out tests

$\rho_{C,Plewe}$ : Radius of relative curvature referring to the test conditions acc. to Plewe

$\rho_{C,test}$ : Radius of relative curvature referring to the carried out tests

$\zeta_{W,Plewe}$ : Wear-effective specific sliding referring to the test conditions acc. to Plewe

$\zeta_{W,test}$ : Wear-effective specific sliding referring to the carried out tests

### 3. Results

#### 3.1. Results of the Nitriding Treatments

The parameters nitriding hardness depth ( $NHD_{400HV}$ ), compound layer thickness ( $CLT$ ), porous zone thickness ( $CLT_p$ ), core hardness, strength as well as the phase composition of the compound layer for the nitrided variants of the test gears are compared in Table 3. Figures 2 and 3 show the hardness curves recorded on the metallographic cross-section and the light microscopic documentation of the compound layers. For the reference, the  $NHD_{400HV}$  is shortly below the targeted value of 0.4 mm, which is due to the somewhat lower quench and temper strength. The compound layer thickness is approx.  $CLT = 11 \mu\text{m}$  including a porous zone of approx.  $CLT_p = 4 \mu\text{m}$ . According to X-ray phase

analysis with chromium radiation, the compound layer consists predominantly of  $\epsilon$ -nitride. In addition, a cementite content of 9% was determined.

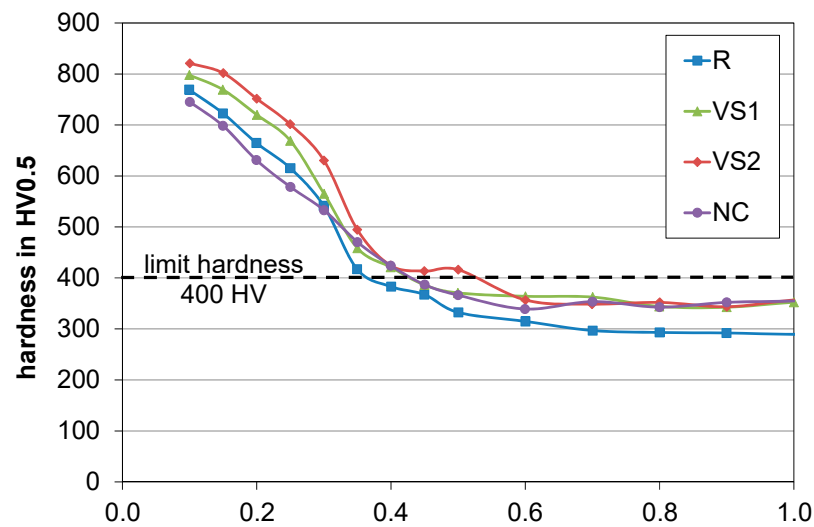


**Figure 2.** Hardness curves of the nitrided layer variants on the material 31CrMoV9.

The compound layers of the three investigated variants VS1, VS2 and NC differ significantly in their thickness, structure and composition (see Table 3 and Figure 3). In variant VS1, a pure  $\gamma'$ -nitride layer was formed according to X-ray phase analysis. Variant VS2 shows also a very high  $\gamma'$ -nitride content. During nitrocarburizing,  $\epsilon$ -nitrides and carbonitrides are formed preferentially due to the additional carbon supply. The phase analysis showed that the  $\epsilon$ -nitride content of the compound layer of the NC variant is significantly greater than in the variants VS1 and VS2, but that the layer nevertheless is a mixture of  $\gamma'$ -nitride and  $\epsilon$ -nitride.

The nitriding hardness depth of VS2 appears to be higher than that of the VS1 and NC treatments. When comparing the hardness depth curves (see Figure 2), it is clear that the different nitriding hardness depth is due to variations in the range of the limiting hardness of 400 HV0.5. Overall, it can be stated that these three variants exhibit a nitriding hardness depth comparable to the reference. As expected, the hardness of the variant NC up to a depth of approx. 0.3 mm is lower compared to the variants VS1 and VS2 due to the higher treatment temperature. Compared with the reference state, where a lower heat-treatable strength was already present before nitriding, there is hardly any difference between the variants VS1, VS2 and NC.

Instrumented indentation testing was used to determine the hardness of the compound layer and the porous zone. According to Table 4 similar hardness values were determined within the compact compound layers. The differences are in the range of the standard deviation, so it is difficult to make statements regarding the differences. The hardness of the porous zone could only be determined for the NC variant. Here it can be seen that, due to its structure, it is somewhat softer than the pore-free part of the compound layer.

**Table 4.** Micro-hardness (testing force 5 mN) of the compound layers.

Variant	Location	Hardness HV	Standard Deviation
R (reference) 510 °C 30 h	Compact compound layer	1049	53.4
VS1 520 °C 42 h $K_N = 1$	Compact compound layer	1094	90.4
VS2 520 °C 42 h $K_N = 3$	Compact compound layer	1158	79.8
NC 550 °C 21 h $K_N = 1$ $K_C^B = 0.1$	Compact compound layer	1032	24.7
	Porous zone	914	39.3



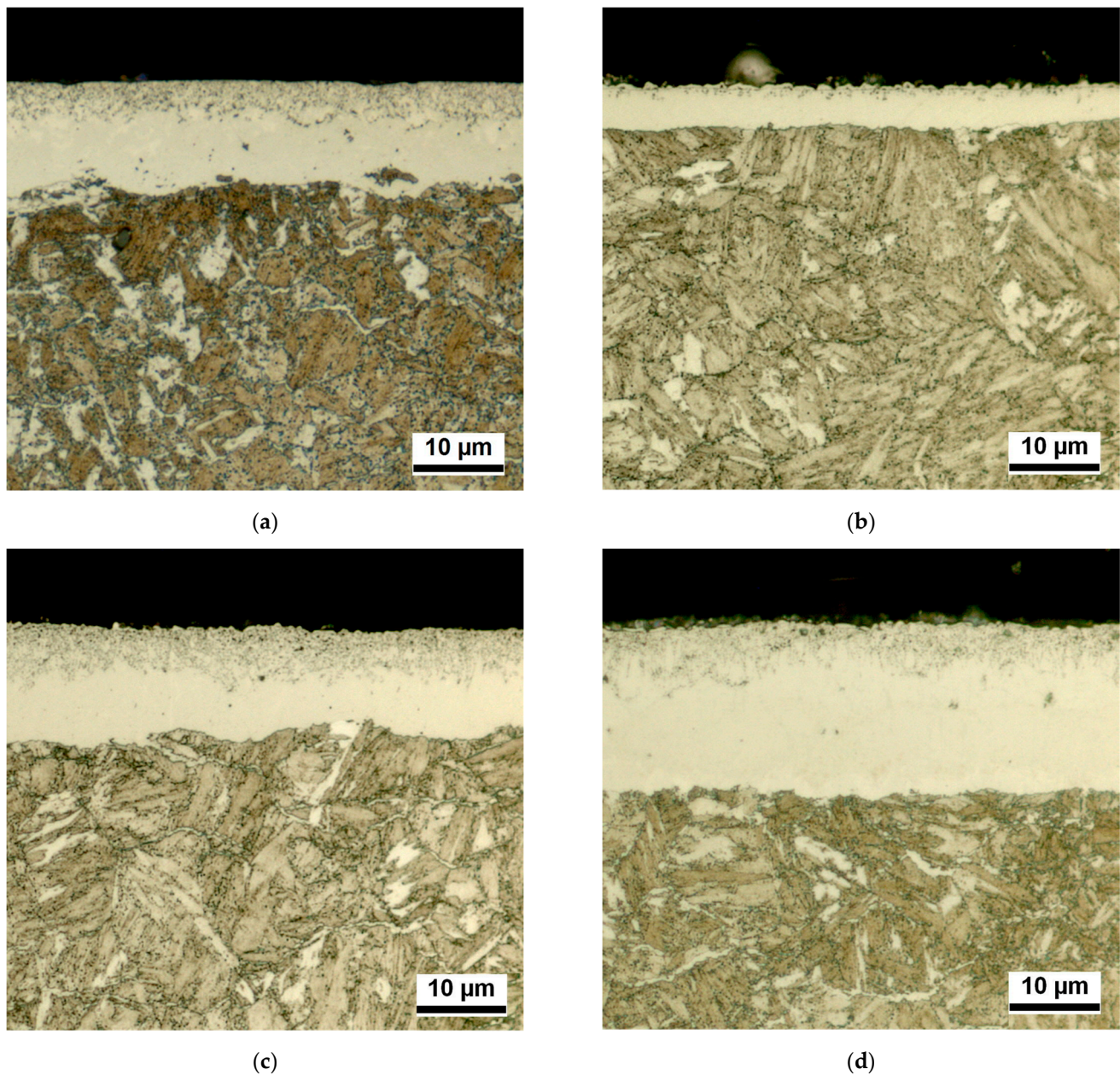


**Figure 3.** Microstructure of the compound layers on material 31CrMoV9 in cross-sections etched with Nital (1000:1): (a) R (reference), 510 °C 30 h; (b) VS1, 520 °C 42 h  $K_N = 1$ ; (c) VS2, 520 °C 42 h  $K_N = 3$ ; (d) NC, 550 °C 21 h  $K_N = 1$   $K_C^B = 0.1$ .

### 3.2. Results within the Load Stage Tests

On the reference test wheels, damages to the compound layer occurred. The damage always started from the tip edge of the test wheel (beginning of contact). From loads of  $p_C^* = 1100 \text{ N/mm}^2$ , there were initially isolated areas with a spalled compound layer respectively white layer flaking, so-called according to ISO/TR 10825 [31] (see Figure 4a). As the load stage test progressed, both the number of affected teeth and, in some cases, the extent of the damage increased. From a pressure of  $p_C^* = 1700 \text{ N/mm}^2$ , a narrow matt gray zone could be observed in the dedendum flank close to the tooth root of the pinion (see Figure 4b). A detailed analysis of this area under the scanning electron microscope shows that the damage is comparable to typical micro-pitting (see Figure 4c) known from case-hardened gears.

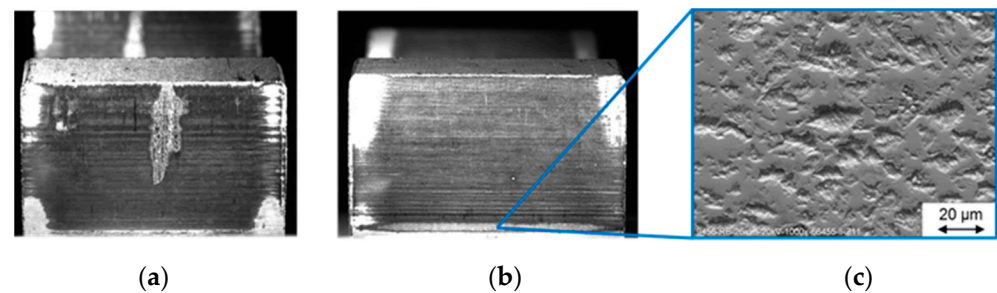


**Figure 4.** Exemplary flank photos of test wheel (a) and test pinion (b) of the reference R after end of test in the load stage test as well as SEM images of micro-pitting (c).

The influence of the thickness and composition of the compound layer on the micro-pitting behavior was investigated using the variants VS1 (thin compound layer,  $\gamma'$ -nitride), VS2 (thick compound layer,  $\gamma'$ -/ $\epsilon$ -nitride) and NC (thick compound layer,  $\gamma'$ -/ $\epsilon$ -nitride) with comparable nitriding hardness depth.

For variant VS1, micro-pitting occurred in the dedendum area of the test pinion from a load of  $p_C^* = 1550 \text{ N/mm}^2$ , and thus one load level earlier than in the reference. At the highest load level ( $p_C^* = 1850 \text{ N/mm}^2$ ), micro-pitting then also appeared in the area of the tip edge of the test pinion of variant VS1 (see Figure 5a). Variant VS1 is the only variant examined here, which spalling of the compound layer on the tooth flanks of the test gears could not be observed for. From a load of  $p_C^* = 1700 \text{ N/mm}^2$ , unlike the reference, micro-pitting could be observed on variant VS1 in the dedendum of the test wheel (see Figure 5b).

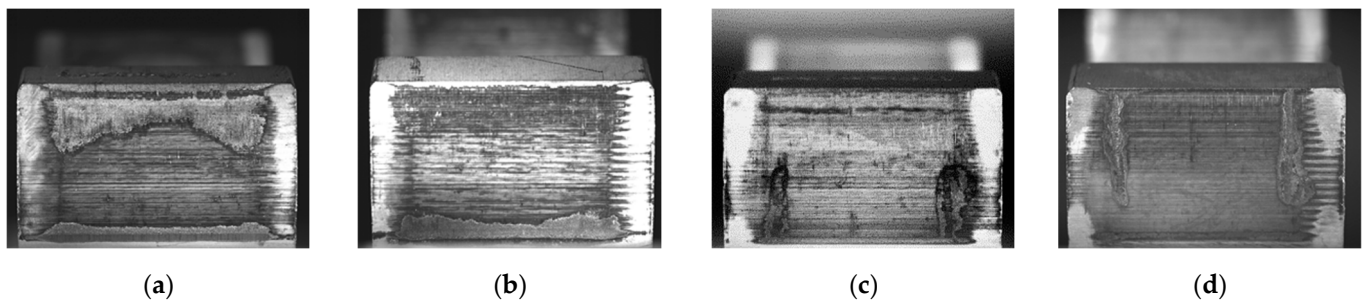


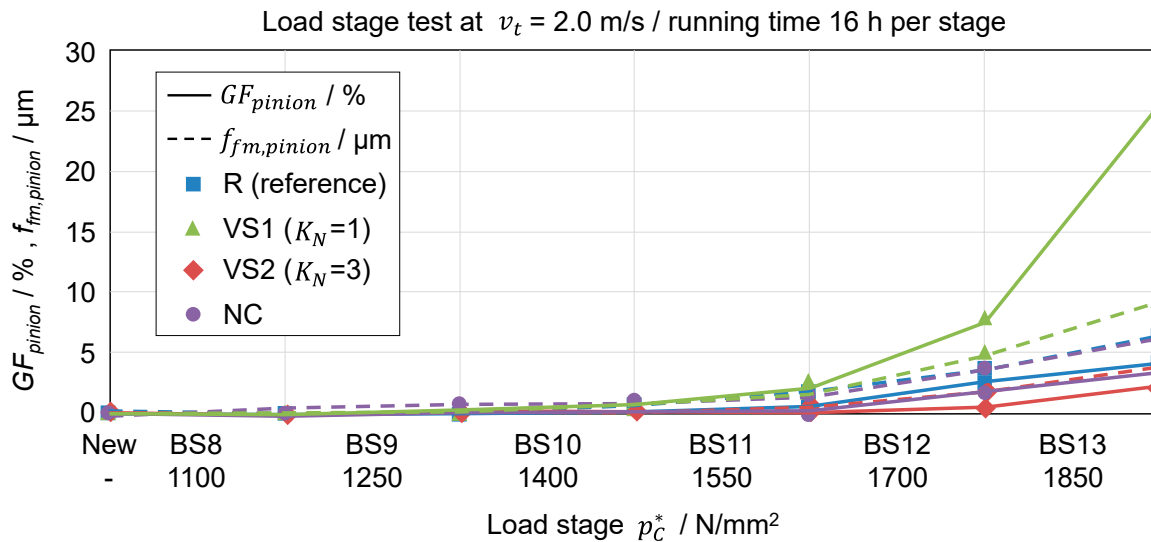
**Figure 5.** Exemplary flank photos after the end of the load stage test: (a) test pinion of variant VS1; (b) test wheel of variant VS1; (c) test pinion of variant NC; (d) test wheel of variant NC.

No micro-pitting was observed on the tooth flanks of the test gears of variant VS2 in the first test run. The spalling of the compound layer on the tooth flanks of the test wheels occurred only from loads of  $p_C^* = 1700 \text{ N/mm}^2$  and was significantly less distinct compared to the reference. In the second test run, the damage to the compound layer already occurred from loads of  $p_C^* = 1400 \text{ N/mm}^2$  and with a stronger extent. From a load of  $p_C^* = 1700 \text{ N/mm}^2$ , slight micro-pitting on the pinion here could be detected on this variant VS2.

On the nitrocarburized NC variant, spalling of the compound layer starting from the tip edge of the test wheels was observed from a load of  $p_C^* = 1400 \text{ N/mm}^2$  in the load stage test. Micro-pitting was observed on the tooth flanks of the test pinions from a load of  $p_C^* = 1700 \text{ N/mm}^2$ . The micro-pitting was concentrated mainly on a very narrow flank area close to the tooth root flank of the test pinions (see Figure 5c) and on areas in contact with damaged parts of the corresponding wheel flank (see Figure 5d).

Figure 6 shows the development of the micro-pitted area  $GF$  and the average profile deviation  $f_{fm}$  on the test pinion of the compound layer variants VS1, VS2 and NC in comparison with the reference. Both the micro-pitted area and the average profile deviation on the pinion of variant VS1 are slightly above the values of the reference up to the highest

load level. The strong increase in the micro-pitted area, with a significantly less extended increase in the profile deviation of this variant in the last stage BS13, is due to the additional micro-pitting that occurred in the area of the tip flank. In contrast to the variant VS2 and the reference, the variant VS1, which was characterized by only a very thin porous zone ( $CLT_P \approx 0.5 \mu\text{m}$ ) before testing, already shows more micro-pitting with very small profile deviations. With regard to the micro-pitting behavior, the VS2 variant benefits from a more extended and continuous porous zone of the compound layer.



#### Test conditions

Lubricant: FVA3 + 4 % Anglamol 99

$Ra_{pinion} \approx 0.25 - 0.29 \mu\text{m}$

Injection lubrication:  $\vartheta_{oil} = 60 \text{ }^\circ\text{C}$

$Ra_{wheel} \approx 0.24 - 0.27 \mu\text{m}$

**Figure 6.** Micro-pitted area  $GF_{pinion}$  and profile deviation  $f_{fm, pinion}$  of the test pinion of the variants VS1, VS2 and NC compared to the reference in the course of the load stage test.

The NC variant confirms that initially profile deviations without observing micro-pitting are measured in the dedendum flank area of the test pinions. Only when the profile deviation is comparable to the magnitude of the porous zone thickness  $CLT_P$  of the respective variants or above, micro-pitting can be observed on the tooth flanks. The nitrocarburized NC variant with a compound layer of about 50%  $\epsilon$ -carbonitride shows a comparable micro-pitting behavior to the reference, whose compound layer also consists of approx. 50%  $\epsilon$ -nitride.

Irrespective of the roughness in the as-nitrided condition, the test pinions and wheels of all compound layer variants show comparable roughness values of  $R_a$  after a partly significant smoothing ( $\Delta R_a \approx 0.05 \dots -0.1 \mu\text{m}$ ) within the first load stage BS 8. Only the test pinion of the variant VS1 shows a slight increase in surface roughness in the final load stage BS 13 due to the strongly increasing micro-pitted area.

With regard to the shown results, it is to be noted that only very limited numbers of load cycles were completed within the load stage tests with a running time of 16 h per stage. The results indicate that the presence of a porous zone has a decisive influence on the micro-pitting behavior of nitrided gears. Therefore, it cannot be excluded that longer running times will completely remove the porous zone resulting in stronger formation of micro-pitting. However, in case that the load does not lead to the erosion of the porous zone, it can be assumed that micro-pitting on nitrided gears can be avoided even for long running times.

### 3.3. Results from the Speed Stage Test

After running-in effects within the first speed stage GS 1, the reference showed almost no optical change in the tooth flanks up to a circumferential speed of  $v_t = 0.25$  m/s. In contrast to comparable investigations on case-hardened gears [27], micro-pitting could here not be detected. At circumferential speeds of  $v_t < 0.25$  m/s, a transition to a wear-related damage of the nitrided tooth flanks was observed, particularly in the areas above and below the pitch circle of the test pinion and wheel.

The measurements of the profile shape (see Figure 7) show that the impact of the contact begin already causes a noticeable profile deviation in the flank area near the tooth root of the nitrided test pinion within the first speed stage GS 1 ( $v_t = 2$  m/s). Up to a circumferential speed of  $v_t = 0.25$  m/s, no significant change in this flank shape could be detected. Only from circumferential speeds of  $v_t < 0.25$  m/s, a further increase in material removal on the flank surface was observed.

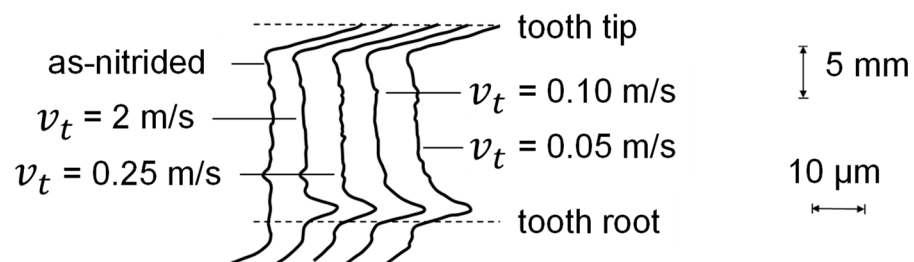
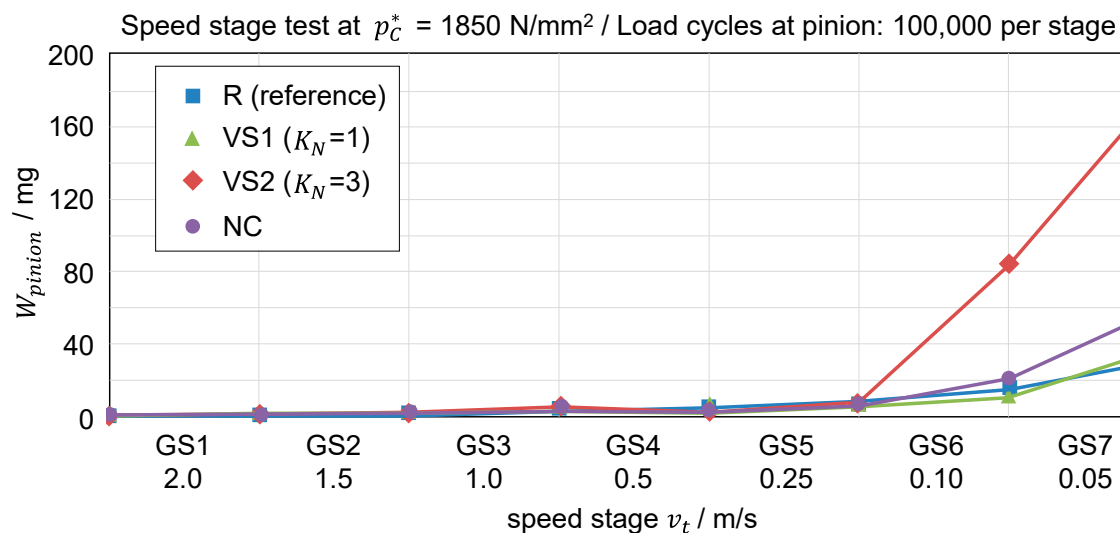


**Figure 7.** Exemplary measurements of the profile shape of the test pinion of the reference in the course of the speed stage test.

This transition to a wear-related damage can also be seen in the course of the mass loss  $W_{pinion}$  on the test pinions (see Figure 8). From circumferential speeds of  $v_t < 0.25$  m/s, a noticeable decrease of the pinions' mass for all variants can be seen.



#### Test conditions

Lubricant: FVA3

Injection lubrication:  $\vartheta_{oil} = 60$  °C

$Ra_{pinion} \approx 0.29 - 0.33$  μm

$Ra_{wheel} \approx 0.23 - 0.35$  μm

**Figure 8.** Cumulated mass wear amounts  $W_{pinion}$  of the nitrided test pinions of the variants R, VS1, VS2 and NC in the speed stage test, revaluated to equal numbers of load cycles per speed stage.

To determine the influence of the thickness and composition of the compound layer on the wear behavior, the compound layer variants VS1, VS2 and NC are plotted in comparison

with the reference in Figure 8. On variant VS1, a thin compound layer consisting only of less hard  $\gamma'$ -nitride was generated via a nitriding potential  $K_N = 1$ . In the course of the speed stage test on the test pinion, this variant shows a mass loss  $W_{pinion}$  comparable to the reference. In contrast, on the test pinion of variant VS2, with a thicker compound layer consisting to a small extent of  $\epsilon$ -nitride (15%), a very strong increase in the amounts of  $W_{pinion}$  was observed from circumferential speeds of  $v_t < 0.25$  m/s.

The wear amounts determined at circumferential speeds of  $v_t \geq 0.10$  m/s on the nitrocarburized variant NC are in the range of the reference. In the last speed stage GS 7 ( $v_t = 0.05$  m/s), a slight increase in mass loss was observed.

The profile deviations of the VS1 and VS2 variants were comparable with the reference. Only at the test pinions of the NC variant were slightly larger profile deviations measured from the beginning. The high mass loss of the variant VS2 is also represented in a strong increase of the profile deviation from a circumferential speed of  $v_t = 0.25$  m/s (GS 5) onwards. On the test pinions of the variant VS1, on the other hand, almost no further change in the profile shape could be detected even at the lowest circumferential speeds.

## 4. Discussion

### 4.1. Micro-Pitting Behavior

With regard to the tested nitrided variants, a correlation was found between the micro-pitted area  $GF_{pinion}$  and the assumed remaining porous zone thickness of the nitrided test pinion, which was determined as the difference between the average profile deviation  $f_{fm, pinion}$  measured after the corresponding test interval and the porous zone thickness  $CLT_P$  before testing, as-nitrided. The analysis (see Figure 9) shows that no significant micro-pitting occurs as long as there is still a sufficient porous zone thickness available on the tooth flank. (Note: Inaccuracies in the illustration in Figure 9 are presumably due to local variations in the porous zone thickness and scattering in the determination of the occurring profile deviations.)

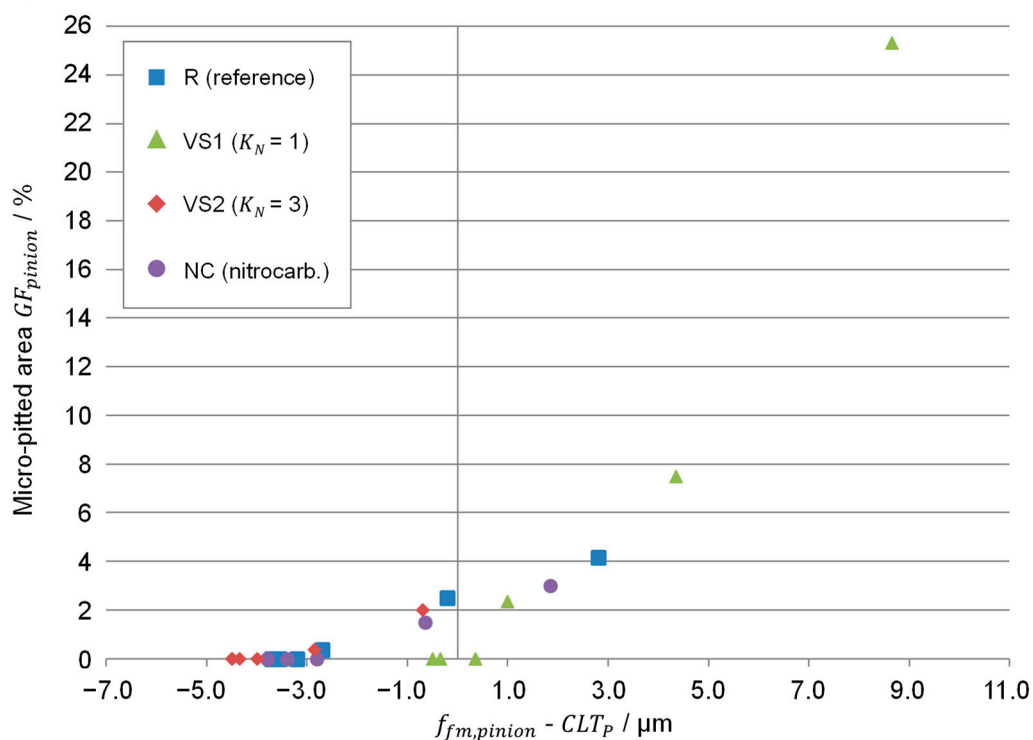


**Figure 9.** Micro-pitted area  $GF_{pinion}$  of the test pinions of the variants investigated in the load stage test as a function of the difference between the profile shape deviation  $f_{fm, pinion}$  measured on the test pinions and the porous zone thickness in the as-nitrided condition  $CLT_P$ .

Crack growth from the surface into the material depth, which is necessary for the formation of micro-pitting, is apparently inhibited in the area of the porous zone. Consequently, the porous zone is first locally removed before micro-pitting formation can start in the compound layer.

In closed compound layers of only  $\epsilon$ -nitride, tensile residual stresses are typically shown near the surface. With increasing distance from the surface, these change to compressive residual stresses. In contrast, residual compressive stresses are always occurring at the surface of compound layers of only  $\gamma'$ -nitride and in  $\gamma'$ - $\epsilon$ -mixed layers. These residual compressive stresses can be as high as  $-700$  to  $-800$  MPa for the material 31CrMoV9 [32]. According to [33], high surface hardness and high residual compressive stresses can help prevent surface cracking (and consequently the formation of micro-pitting). Compound layers consisting predominantly of the harder  $\epsilon$ -nitride are supposed to be characterized by less at risk in terms of micro-pitting than compound layers containing only less hard  $\gamma'$ -nitride. Accordingly, the variant VS1 with a compound layer of 100%  $\gamma'$ -nitride shows a significantly stronger micro-pitting development than variants with a compound layer including  $\epsilon$ -nitride (R, VS2 and NC), both with regard to the micro-pitted area and to the profile deviations.

#### 4.2. Wear Behavior

Figure 10 shows a  $h_{C,min}-c_{IT}$  plot according to Plewe [29] including the actual test results and the specific wear curves determined by Plewe for unalloyed mineral oils and the material pairings Eh/Eh (case-hardened/case-hardened) and N/N (nitrided/nitrided). In addition, the wear coefficients determined on internal gears in the pairing Eh/N [34] (case-hardened planets paired with nitrided ring gear variants R, VS1 and VS2—corresponding to the nitrided external gear variants) are illustrated in the plot. All the wear coefficients shown are based in each case on the wear amounts determined for the test pinions (respectively the test planets, which the material losses include the test and drive gearing for [34]). No wear coefficients were calculated for the test wheels due to the occurring spallings of the compound layer (see Figure 4a).

For all nitrided external gear variants, continuously progressive slow-running wear could be detected in the speed stage test with the unadditivated lubricant FVA 3 and at lubricant film thicknesses at the pitch point of  $h_{C,min} < 0.02$   $\mu\text{m}$ . The wear coefficients determined in the course of the speed stage tests for the nitrided external gear variants R, VS1 and NC are ranked between the wear curves according to Plewe for case-hardened and nitrided gearings. Consequently, the scatter range given by Plewe for nitrided gears in the pairing N/N could not be achieved within the tests with lubricant FVA 3. However, this scatter range according to Plewe is based on investigations carried out at significantly lower loads and largely on nitrided gears without a compound layer [29]. Variant VS2 ( $K_N = 3$ ) showed the worst wear behavior for nitrided gears and is ranked more in the scatter range for case-hardened gears in the pairing Eh/Eh according to Plewe.

In comparison, all internal gear variants in the pairing Eh/N [34] are ranked in the scatter range for case-hardened gears according to Plewe. For variant VS2, slightly increased wear coefficients were determined on the case-hardened planet gears compared to variant R and VS1. This tendency considering the wear behavior corresponds to the results of the external gear variants. It can be assumed that gears in the pairing N/N show reduced wear compared to the pairing Eh/N, where mostly the case-hardened specimen is characterized by an increased wear development. Consequently, the results confirm that nitriding can improve the wear behavior of gears compared to other heat treatment processes, such as e.g., case-carburizing.

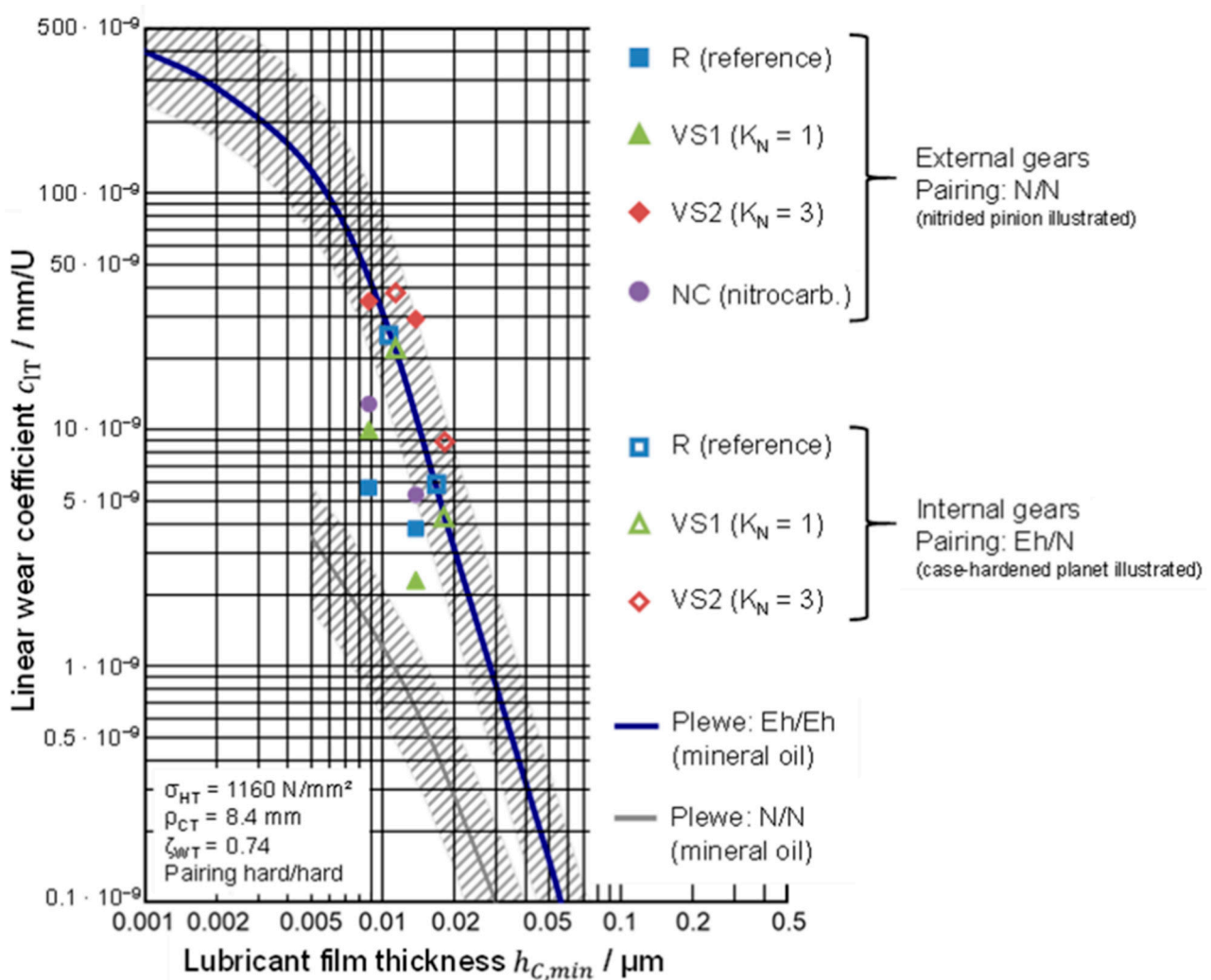


**Figure 10.**  $h_{C,min}$ - $c_{IT}$  plot acc. to Plewe [29] showing the experimental results within the speed stage tests on nitrided external gears in the pairing N/N (and internal gears in the pairing Eh/N [34]).

Influences of compound layer thickness  $CLT$  (in the range of 4.1  $\mu\text{m}$  to 17.6  $\mu\text{m}$ ) or the porous zone thickness  $CLT_P$  (in the range of 0.5  $\mu\text{m}$  to 4.5  $\mu\text{m}$ ) on the wear behavior of external gears in the pairing N/N could not be found on the basis of the results within the speed stage tests. The main influencing factor is supposed to be represented by the composition of the compound layer. A comparison of the mass losses of the test pinions at the end of the test shows that increased wear amounts were determined for variant VS2 with approx. 15%  $\epsilon$ -nitride. The variants with a percentage of approx. 50%  $\epsilon$ -nitride (variants R and NC) and compound layers with 100%  $\gamma'$ -nitride (variant VS1) showed a significantly more favorable wear behavior. The requirements of the standards DIN 3990-5 [17] and ISO 6336-5:2003 [18], according to which a high proportion of  $\epsilon$ -nitride is recommended, are basically supported by these results. In addition, the pure  $\gamma'$ -compound layer of the variant VS1 (also shown for the internal gear variants [34]) appear to have favorable properties with regard to the wear behavior of nitrided gears (but not for micro-pitting, see Chapter 4.1).

#### 4.3. Model of the Damage Mechanism and Damage Development

On the basis of the extensive results of the present research, the basic model concepts for damage initiation and propagation with regard to the damage mechanisms of micro-pitting and slow-running wear on nitrided gears in the pairing N/N were further developed. This is based on the following assumptions and basic ideas.

Micro-pitting could only be detected on nitrided gears when the porous zone in the corresponding areas of the tooth flank was completely removed. With an intact porous zone, initial micro-cracks from the surface hit one of the numerous microscopic cavities after a very short time and cannot propagate any further from there. The porous zone thus initially prevents the formation of micro-pitting until it is completely removed. As soon as there is no longer a continuous porous zone on the surface, micro-pitting can occur in the compound layer. The appearance of micro-pitting on nitrided gears is similar to the typical appearance on case-hardened gears. When micro-pitting occurs on nitrided gears, it develops stronger on compound layers of 100%  $\gamma'$ -nitride than on a surface of  $\epsilon$ -nitride, due to the different structures of the nitrides and stresses. In addition, a porous zone in the  $\epsilon$ -compound layer appears to have higher stability than in a less hard, pure  $\gamma'$ -nitride compound layer. The criterion of a minimum relative lubricant film thickness for assessing the micro-pitting resistance of nitrided gears therefore only applies to nitriding layers without a porous zone. The resistance against the removal of the porous zone, on the other hand, can be influenced by various parameters, such as phase composition of the compound layer and load. However, the properties of the compound layer are primarily decisive for the micro-pitting behavior of nitrided gears.

The results of the experimental investigations have also shown that nitrided gears in the N/N pairing exhibit a significantly more favorable wear behavior than case-hardened gears. This is due to the increased abrasion resistance resulting from the high hardness of the compound layer. In addition, the nitrided surface layer exhibits a reduced coefficient of friction and a reduced adhesion tendency compared to case-hardened gears [35]. A high porous zone thickness does not seem to have a negative influence on continuously progressive low-speed wear. The decisive influence on the wear behavior of nitrided gears therefore is represented by the structure and composition of the compound layer. Compound layers with a high percentage of  $\epsilon$ -nitride (>50%) showed an increased wear resistance. The high proportion of  $\epsilon$ -nitride, which is predominantly present on the material surface, prevents rapid, complete removal of the compound layer. Consequently, the surface offers better wear protection due to the higher hardness of the  $\epsilon$ -phase. However, the investigations have also shown that favorable wear behavior can be achieved with compound layers of pure  $\gamma'$ -nitride. Although the avoidance of the  $\epsilon$ -phase lowers the wear resistance of the nitrided surface, it may also be possible to avoid increased abrasive wear due to the harder particles of  $\epsilon$ -nitride. Significantly stronger wear than for compound layers with approx. 50%  $\epsilon$ -nitride or compound layers of pure  $\gamma'$ -nitride was observed in the pairing N/N (and Eh/N for internal gears) for compound layers with only a limited amount of  $\epsilon$ -nitride (15%). It is assumed that this proportion of  $\epsilon$ -nitride is predominantly present at the surface of the compound layer. Under wear-critical operation conditions, the material removed from the surface initially contains predominantly very hard particles which accumulate in the lubricant, while the surface hardness and wear resistance of the surface decrease as a result of this removal, leading to a noticeable increase in wear.

## 5. Conclusions

In order to investigate the influence of the compound layer on the tribological load carrying capacity of nitrided gears, systematic investigations were carried out on the micro-pitting and wear behavior of nitrided external gears, especially at low circumferential speeds. The main focus was on the variation of the compound layer thickness and phase composition. From the extensive investigations of nitrided external gears in the pairing N/N in load stage and speed stage tests, the following main conclusions could be drawn:

- The compound layer is decisive for the tribological behavior of nitrided gears.
- No micro-pitting could be observed as long as the porous zone was present.
- The wear behavior was not influenced by compound layer or porous zone thickness.
- Compound layers with either 100%  $\gamma'$ -nitride or with a high percentage of  $\epsilon$ -nitride (>50%) showed an increased wear resistance, while only low contents of  $\epsilon$ -nitride have a negative effect on the wear behavior.



A high proportion of  $\epsilon$ -nitride within the compound layer, consequently offers the highest potential for an optimum compromise between wear and micro-pitting resistance. The transferability of the recommendations considering the damage type pitting is currently investigated at FZG and IWT. For applications, in which either only the wear resistance or only the micro-pitting resistance is decisive, compositions of the compound layer deviating from these specifications may offer advantages under certain circumstances.

**Author Contributions:** Conceptualization, S.H., B.Z., F.H. and T.T.; methodology, S.H., B.Z., F.H. and T.T.; validation, S.H., M.G. and B.Z.; investigation, S.H. and B.Z.; resources, F.H., K.S. and R.F.-H.; writing—original draft preparation, S.H., M.G. and B.Z.; writing—review and editing, F.H., T.T., K.S. and R.F.-H.; visualization, S.H., M.G. and B.Z.; supervision, F.H. and T.T.; project administration, S.H. and B.Z.; funding acquisition, F.H., T.T. and K.S. All authors have read and agreed to the published version of the manuscript.

**Funding:** The presented results are based on the research project IGF no. 17730-N/1 (FVA 482/IV) under-taken by the Research Association for Drive Technology e.V. (FVA); supported partly by the FVA and through the German Federation of Industrial Research Associations e.V. (AiF) in the framework of the Industrial Collective Research Programme (IGF) by the Federal Ministry for Economic Affairs and Climate Action (BMWK) based on a decision taken by the German Bundestag. The authors would like to thank for the sponsorship and support received from the FVA, AiF and the members of the project committee.

**Data Availability Statement:** Not applicable.

**Conflicts of Interest:** The authors declare no conflict of interest. The funders had no role in the design of the study; in the collection, analyses, or interpretation of data; in the writing of the manuscript, or in the decision to publish the results.

## References

1. Spies, H.J. Fatigue behavior of nitrided steels. *Steel Res.* **1993**, *64*, 441–448. [[CrossRef](#)]
2. Ebersbach, U. Nitrided/nitrocarburized and oxidized steel: Corrosion data in dependence on the N- and C- content of the E-phase under the oxide layer. In *Passivation of Metals and Semiconductors, and Properties of Thin Oxide Layers, Proceedings of the 9th International Symposium, Paris, France, 27 June–1 July 2005*; Elsevier Science: Amsterdam, The Netherlands, 2006; pp. 715–720.
3. D’Errico, F. Micro-pitting damage mechanism on hardened and tempered, nitrided, and car-burizing steels. *Mater. Manuf. Processes* **2011**, *26*, 7–13. [[CrossRef](#)]
4. Karamis, M. Experimental study of the abrasive wear behavior of plasma-nitrided gearing steel. *Wear* **1993**, *161*, 199–206. [[CrossRef](#)]
5. Spies, H.-J. Controlled gas-nitriding of ferrous materials (German: Kontrolliertes Gasnitrieren von Eisenwerkstoffen). *Stahl* **1992**, *2*, 77.
6. Liedtke, D.; Baudis, U.; Boßlet, J.; Huchel, U.; Lerche, W.; Spies, H.J.; Klümper-Westkamp, H. *Heat Treatment of Ferrous Materials II: Nitriding and Nitrocarburizing (German: Wärmebehandlung von Eisenwerkstoffen II: Nitrieren und Nitrocarburieren)*; Expert Verlag: Renningen, Germany, 2014.
7. Schlötermann, K. Design of Nitrided Gears—Investigations on the Effects of Different Nitriding Parameters on the Material Structure of Gears (German: Auslegung Nitrierter Zahnradgetriebe—Untersuchungen zu den Auswirkungen Unterschiedlicher Nitrierparameter auf den Werkstoffzustand von Zahnrädern). Ph.D. Thesis, RWTH Aachen, Aachen, Germany, 1988.
8. Günther, D.; Pouteau, P.; Bruckmeier, S.; Hoffmann, F.; Oster, P. *Product Safety of Nitrided Gears (German: Nitrierte Zahnräder: Produktsicherheit nitrierter Zahnräder)*; Final report 386 I; Forschungsvereinigung Antriebstechnik e.V.: Frankfurt, Germany, 2005; Volume 777.
9. Schönnenbeck, G. Influence of Lubricants on the Gear Flank Fatigue (Micro-Pitting and Pitting), Mainly for Circumferential Speeds 1...9 m/s (German: Einfluß der Schmierstoffe auf die Zahnflankenermüdung (Graufleckigkeit und Grübchenbildung) hauptsächlich im Umfangsgeschwindigkeitsbereich 1...9 m/s). Ph.D. Thesis, TU München, München, Germany, 1984.
10. Emmert, S. Investigations on the Gear Flank Fatigue (Micro-Pitting, Pitting) of High Speed Gear Transmissions (German: Untersuchungen zur Zahnflankenermüdung (Graufleckigkeit, Grübchenbildung) Schnellaufender Stirnradgetriebe). Ph.D. Thesis, TU München, München, Germany, 1994.
11. Bull, S.; Evans, J.; Shaw, B.; Hoffmann, D. The effect of the white layer on micro-pitting and surface contact fatigue failure of nitrided gears. *Proc. Inst. Mech. Eng. Part J J. Eng. Tribol.* **1999**, *213*, 305–313. [[CrossRef](#)]
12. Goman, A.; Kukareko, V. Contact endurance of gearing teeth subjected to ion-beam nitriding. *J. Mach. Manuf. Reliab.* **2014**, *43*, 69–74. [[CrossRef](#)]

13. Le, M.; Ville, F.; Kleber, X.; Cavoret, J.; Sainte-Catherine, M.C.; Briancon, L. Influence of grain boundary cementite induced by gas nitriding on the rolling contact fatigue of alloyed steels for gears. *Proc. Inst. Mech. Eng. Part J J. Eng. Tribol.* **2015**, *229*, 917–928. [[CrossRef](#)]
14. Sitzmann, A.; Tobie, T.; Stahl, K.; Schurer, S. Influence of the Case Properties after Nitriding on the Load Carrying Capacity of Highly Loaded Gears. In Proceedings of the ASME Proceedings, IDETC2019-97405. Anaheim, CA, USA, 18–21 August 2019.
15. Sitzmann, A.; Hoja, S.; Schurer, S.; Tobie, T.; Stahl, K. Deep nitriding—Contact and bending strength of gears with increased. *Forschung im Ingenieurwesen* **2021**. [[CrossRef](#)]
16. Xu, H.; Li, H.; Hu, J.; Wang, S. A study on contact fatigue performance of nitrided and tin coated gears. *Adv. Mater. Sci. Eng.* **2013**, *2013*, 580470. [[CrossRef](#)]
17. *DIN 3990-5; Calculation of Load Capacity of Cylindrical Gears—Part 5: Endurance Limits and Material Qualities (German: Tragfähigkeitsberechnung von Stirnrädern—Teil 5: Dauerfestigkeitswerte und Werkstoffqualitäten)*. Beuth-Verlag: Berlin, Germany, 1987.
18. *ISO 6336-5; Calculation of Load Capacity of Spur and Helical Gears—Part 5: Strength and Quality of Materials*. Beuth-Verlag: Berlin, Germany, 2003.
19. *ISO 6336-5; Calculation of Load Capacity of Spur and Helical Gears—Part 5: Strength and Quality of Materials*. Beuth-Verlag: Berlin, Germany, 2016.
20. *DIN 30902:2016-12; Heat Treatment of Ferrous Materials—Light-Microscopical Determination of the Depth and Porosity of the Compound Layer of Nitrided and Nitro-Carburized Ferrous parts. (German: Wärmebehandlung von Eisenwerkstoffen—Lichtmikroskopische Bestimmung der Dicke und Porosität der Verbindungsschichten Nitrierter und Nitrocarburierter Werkstücke)*. Beuth-Verlag: Berlin, Germany, 2016.
21. *ISO 18265; Metallic Materials—Conversion of Hardness Values*. Beuth-Verlag: Berlin, Germany, 2013.
22. Epp, J. *XRD Methods for Materials Characterization in Material Characterization Using Nondestructive Evaluation (NDE) Methods*; Woodhead Publishing: Cambridge, UK, 2016; pp. 81–124.
23. *ISO 6336-1; Calculation of Load Capacity of Spur and Helical Gears—Part 1: Basic Principles, Introduction and General Influence Factors*. Beuth-Verlag: Berlin, Germany, 2019.
24. Zornek, B. Investigations on the Flank Load Carrying Capacity of Through-Hardened and Nitrided Internal and External Gears (German: Untersuchungen zur Flankentragfähigkeit vergüteter und nitrierter Innen- und Außenverzahnungen). Ph.D. Thesis, TU München, München, Germany, 2018.
25. *DIN 3963; Tolerances for Cylindrical Gear Teeth; Tolerances for Working Deviations (German: Toleranzen für Stirnradverzahnungen: Toleranzen für Wälzabweichungen)*. Beuth-Verlag: Berlin, Germany, 1978.
26. *DIN ISO 14635-1; Gears-FZG Test Procedures—Part 1: FZG Test Method A/8,3/90 for Relative Scuffing Load-Carrying Capacity of Oils (German: Zahnräder—FZG-Prüfverfahren—Teil 1: FZG-Prüfverfahren A/8,3/90 zur Bestimmung der Relativen Fresstragfähigkeit von Schmierölen)*. Beuth-Verlag: Berlin, Germany, 2006.
27. Schudy, J.; Tobie, T.; Höhn, B.-R. *Flank Load Carrying Capacity of Internal and External Cylindrical Gears at Low Circumferential Speeds (German: Flankentragfähigkeit von Innen- und Außenverzahnungen bei Geringen Umfangsgeschwindigkeiten)*; Final report FVA 482/I; Forschungsvereinigung Antriebstechnik e.V.: Frankfurt, Germany, 2008; Volume 867.
28. Emmert, S.; Schönnenbeck, G.; Oster, P.; Rettig, H. *FVA-Informationsblatt Nr. 54/7: Micro-Pitting Test (German: Graufleckentest) C/8,3/90*; Forschungsvereinigung Antriebstechnik e.V.: Frankfurt, Germany, 1993.
29. Plewe, H.-J. Investigations on the Wear of Lubricated Slow-Speed Running Gears (German: Untersuchungen über den Abriebverschleiß von Geschierten, Langsam Laufenden Zahnradern). Ph.D. Thesis, TU München, München, Germany, 1980.
30. Dowson, D.; Higginson, G.R. *Elasto-Hydrodynamic Lubrication—The Fundamentals of Roller Gear Lubrication*; Pergamon Press Oxford: Oxford, UK, 1966.
31. *ISO/TR 10825-2 (DRAFT); Gears: Wear and Damage to Gear Teeth—Part 2: Supplementary Information*. Beuth-Verlag: Berlin, Germany, 2021.
32. Oettel, H.; Ehrentraut, B. Makroscopic residual stresses in the compound layer of gas-nitrided steels (German: Makroskopische Eigenspannungen in der Verbindungsschicht gasnitrierter Stähle). *HTM J. Heat Treat. Mater.* **1985**, *40*, 183–187. [[CrossRef](#)]
33. Trubitz, P.; Spies, H.-J. Fatigue behavior of nitrided steels (German: Ermüdungsverhalten nitrierter Stähle). *HTM J. Heat Treat. Mater.* **1996**, *51*, 378–384.
34. Geitner, M.; Zornek, B.; Hoja, S.; Tobie, T.; Stahl, K. Investigations on the Micro-Pitting and Wear Behavior of Nitrided Internal Gears. *IOP Conf. Ser. Mater. Sci. Eng.* **2021**, *1097*, 012005. [[CrossRef](#)]
35. Zoch, H.-W.; Spur, G. *Handbook Heat Treatment and Coating (German: Handbuch Wärmebehandeln und Beschichten)*; Carl Hanser Verlag: München, Germany, 2015.